Bulletin of Environmental Contamination and Toxicology (2022) 109:122–129
https://doi.org/10.1007/s00128-022-03493-8

Spatial Characteristics and Risk Assessment of Heavy Metals in the Soil-Vegetation System of a Red Mud Slag Yard, SW China

Runyu Zhang[1] · Zhi Zhang[1,2] · Jing Wu[1,2] · Liying Wang[1]

Received: 24 December 2021 / Accepted: 17 February 2022 / Published online: 4 March 2022

Abstract

The purpose of this study was to investigate the distribution pattern, pollution status and potential ecological risk of Cr, Co, Ni, Cu, As, Cd, Sb, and Pb in soils and dominant plants around an abandoned red mud (RM) slag yard in Southwestern China. Soils exhibited representative enrichment and combination characteristics of these metals compared to the background values, ascribed to the leaching of long-term acid rain on the RM dump. The soil was moderately to severely polluted with As and Sb. Cd also posed a moderate ecological risk. Asteraceae species predominated in the RM slag yard, followed by *Coriaria sinica* and *Robinia pseudoacacia*. No plants were identified as hyperaccumulators because of low bioconcentration values, whereas *Cosmos bipinnata* can act as a potential phytostabilizer of heavy metals based on the translocation factor. The results provided effective decision support for reducing heavy metal pollution by phytoremediation RM stacking fields.

Keywords Bauxite residue disposal field · Heavy metal · Soil-vegetation system · Potential ecological risk · Phytoremediation

Aluminum (Al), as the third most abundant element in the Earth's crust, is widely used in the packaging, transportation, construction and industrial sectors owing to its versatile properties (Mayes et al. 2016). Increasing consumption of aluminum has resulted in the expansion of bauxite mining activities along with the massive emission of bauxite residue, namely, red mud (RM), which is a hazardous solid waste produced during alumina production. To date, four billion tons of RM is estimated to be discharged from aluminum industries and stockpiled worldwide, posing a huge threat to the ambient environment (Mayes et al. 2016; Ren et al. 2018).

China is the major producer of alumina, and it has discharged approximately 0.6 billion tons of RM at an annual growth rate of 70 million tons (Xue et al. 2016). However, the treatment of RM is a challenge because of its huge stockpile. It is estimated that only 10% of RM could be reused, and the rest relies on dam storage (Ujaczki et al. 2018). Hence, RM is potentially hazardous to the eco-environment due to its high alkalinity, causticity and enrichment of potentially toxic substances, e.g., heavy metals and radionuclides (Ghosh et al. 2011; Xue et al. 2016; Ren et al. 2018; Gautam and Agrawal 2019).

As previously mentioned, the migration and enrichment of heavy metals to the eco-environment from the RM slag yard is of great concern to the public because of their toxic, persistent, and bioaccumulative nature. RM generally contains As, Cd, Cr, Co, Mn, Ni, Zn, Cu, and Pb (Ghosh et al. 2011; Ren et al. 2018). Upon contact with water, the mobility of oxyanions forming trace elements (e.g., Al, As, Cr, Mo and V) in RM is expected to increase greatly (Mišík et al. 2014; Yang et al. 2021). Furthermore, the leaching and deposition of heavy metals through the eluviation of rainfall can indirectly affect nearby water body safety, soil quality and vegetation. Recent studies have conducted ecological risk assessments of soil heavy metals in the main RM slag yards from Henan and Guangxi Provinces, China (Sun et al. 2015; Guo et al. 2018). Although these studies almost focused on the risk evaluation of soil heavy metals in the RM dumping yard, limited efforts have been made to investigate the bioaccumulation potentiality of these toxic elements in

✉ Runyu Zhang
zhangrunyu@vip.gyig.ac.cn

[1] State Key Laboratory of Environmental Geochemistry, Institute of Geochemistry Chinese Academy of Sciences, Guiyang 550081, Guizhou, China

[2] University of Chinese Academy of Sciences, Beijing 100049, China

the food chain via plant uptake (e.g., Mišík et al. 2014; Di Carlo et al. 2019).

At present, the use of suitable plants for removing or accumulating heavy metals in the RM stack field is a promising technique (Courtney et al. 2009; Mishra et al. 2017; Gautam et al. 2018; Di Carlo et al. 2019). A series of field-established rehabilitation strategies reflecting both direct revegetation and revegetation on the capping layer or with amendments were assessed in terms of both soil and plant quality (Courtney et al. 2009; Chauhan and Ganguly 2011; Xue et al. 2016; Gautam and Agrawal, 2019). Di Carlo et al. (2019) found that vegetation excessively took up Al, Na, Fe, Cr and V in a long-term bauxite residue remediation program. Moreover, plants can translocate these elements to their shoots at high concentrations (Di Carlo et al. 2020). A good candidate plant for phytomanagement should have a high biomass, fast growth rate, metal tolerance and high metal accumulation capacity in its aboveground tissues (Courtney et al. 2009; Burges et al. 2018), and herbaceous species have been recommended as priorities for most present studies (Chauhan and Ganguly 2011; Xue et al. 2016; Gautam et al. 2018). However, the potential for heavy metal uptake and phytotoxicity in revegetated RM slag yards has been largely unreported.

In light of the abovementioned issues, we performed an integrated study at an abandoned RM slag yard in Guizhou Province, Southwestern China, which is well known for bauxite mining and alumina processing. The principal objectives of this study were to 1) investigate the spatial variability and contamination level of heavy metals (Cr, Co, Ni, Cu, As, Cd, Sb, and Pb) in the soils around this RM dumping yard; (2) evaluate the potential eco-environmental risk of selected heavy metals; and (3) clarify the accumulating and transfer capacity of these toxic elements by regional vegetation based on translocation (*TF*) and bioconcentration (*BCF*) factors.

Materials and Methods

An abandoned alumina factory (106°35′18″ E, 26°41′27″ N) located 17 km NW of Guiyang city, the capital of Guizhou Province, China, was selected as the study area (Fig. S1). The factory has been operated for more than 30 years. It initially produced approximately 220,000 tons/year of alumina by using the Bayer process and then an additional 180,000 t/a alumina production scale was expanded by adopting a sintering process in the second-phase project. Afterwards, the combined production process was put into operation with a total alumina production of 400,000 t/a. The aluminum factory was completely shut down in 2014, and the RM slag yard was completely closed in 2018. The climate of this study area is a subtropical rainy monsoon. It has an annual average rainfall of 1110 mm, and most of the precipitation concentrates from May to October. The RM dump dam covered an area of 660,000 m^2, with a height of 79 m and a total storage capacity of more than 23 million m^3. The dam was renovated, top-hardened, and revegetated around the cofferdam. The side slope of the RM disposal area was capped with a thin soil layer to support plant colonization. A few shrubs and grass are found around the RM disposal field.

Three kinds of RM samples from the Bayer process, sintering process, and combined Bayer-sintering process before 2014 were taken from the slag yard. Surface soil samples (0–15 cm) were collected from eight sites at one side slope of the RM disposal field in 2020. Among them, 4 locations (including $1^{\#}$, $3^{\#}$, $5^{\#}$, and $7^{\#}$) are situated in the upper part of the slope, and the rest (including $2^{\#}$, $4^{\#}$, $6^{\#}$, and $8^{\#}$) lie in the lower part. Approximately 3–5 subsamples were gathered at random within a 5-m radius for each sampling site and mixed well to guarantee sample representativeness. Around each soil sampling point, dominant plant species, such as herbs, shrubs and trees, were collected separately. Plant species were identified mainly as *Artemisia argyi*, *Conyza canadensis*, *Buddleja lindleyana*, *Cosmos bipinnata, Coriaria sinica*, *and Robinia pseudoacacia* using classical morphological and taxonomic identification methods, with reference to Flora Reipublicae Popularis Sinicae (Flora of China 2014). All samples were sealed in plastic bags and then shipped back to the laboratory.

In the laboratory, visible root residues and stone debris were manually removed from soil samples and then air-dried alongside RM samples. Soils were divided into two subsamples: one was passed through a 2 mm nylon sieve for physicochemical property analysis, and the other was ground to 100 mesh for heavy metal determination. Fresh plant organs, including shoots, stems and leaves, were separated and carefully washed with deionized water and then completely dried at 90 °C for 24–48 h in an oven. Furthermore, dried plant subsamples were ground into powder using an agate mortar and stored in a desiccator.

The pH values of RM and soil samples were measured in a 1:5 (w/v) aqueous extract using a digital pH meter. The moisture content was calculated when dried at 105 °C to a constant weight. For heavy metal analysis, RM, soils, and plant tissues were digested with a mixture of concentrated HNO_3 and HF. All digested solutions were filtered with a 0.45 μm cellulose acetate membrane and then diluted with deionized water to 50 ml for analysis. The heavy metal contents (Cr, Co, Ni, Cu, As, Cd, Sb, Pb) in the supernatants were determined using plasma mass spectrometry (ICP–MS, Agilent HPLC1290-7700x, USA). Reagent blanks, duplicate samples and standard reference materials (GBW07407/GSS-7, Latosol) supplied by IGGE at the Chinese Academy of Geological Sciences were used to analyze the quality assurance and quality control. The recoveries of selected heavy metals ranged from 94.4 to 110.5% at the 95% confidence level. The reagents and standard solutions used were of guarantee grade.

Additionally, heavy metal contamination in soils was comprehensively evaluated by the single and comprehensive Nemerow pollution indices (P_i and P_N) and the potential ecological risk index (*RI*). More detailed information can be found in Supplementary Content Text S1, while the categories of P_i, P_N, and RI are given in Tables S1 and S2. The plant fixation and accumulation abilities of different heavy metals were also assessed by using bioconcentration (*BCF*), and translocation (*TF*) factors were calculated (Gautam and Agrawal 2019; Inzar-Sekuli et al. 2019). In this study, TF_1 was further expanded to compare the transfer efficiency of heavy metals between the underground part and the aerial part. They can be calculated by Eqs. (1), (2) and (3):

$$\mathrm{BCF} = \frac{\text{Metal content in plant tissue}}{\text{Metal content in soil}} \tag{1}$$

$$\mathrm{TF} = \frac{\text{Metal content in stem tissue}}{\text{Metal content in root tissue}} \tag{2}$$

$$\mathrm{TF}_1 = \frac{\text{Metal content in leaf tissue}}{\text{Metal content in stem tissue}} \tag{3}$$

Statistical analysis was carried out by SPSS version 22.0. Descriptive statistics were used to describe the metal levels in the samples. Spearman correlation analysis was conducted to determine the relationship between different heavy metal contents in samples. All data were plotted using Origin software (version 8.1).

Results and Discussion

The basic physicochemical characteristics of typical RM samples from Guizhou Aluminum Company are summarized in Table S3. The pH values of the RM samples varied from 9.79 to 11.03, indicating a strongly alkaline nature. For the moisture content, the Bayer RM has a higher ratio than the other two types of RM. All RM samples consisted mainly of Al_2O_3, S_iO_2, Fe_2O_3, CaO, TiO_2, Na_2O, K_2O and MgO. The total contents of the selected heavy metals in these RM samples are listed in Table 1. The trace element compositions varied slightly among the three kinds of RM and ranked in a decreasing order of Cr > Pb, Cu > Ni > As > Co > Sb > Cd. As raw materials for alumina production, some heavy metals are inherently rich in bauxite ore. In essence, bauxite ore is generally formed from the intense lateritic weathering of residual clays, which accumulate in topographic lows on continental surfaces (Ahmadnejad et al. 2017). Trace elements, including REEs, Ti, Zr, Cr and As, can be adsorbed onto the surface of residual clays and then become concentrated with depth in the resulting bauxite deposits. The bauxite grade and the efficiency of the alumina extraction process also affected the production of alumina and the generation of RM. The production of each tone of alumina usually consumes approximately 1.8–2.6 tons of bauxite and produces approximately 1–1.5 tons of RM. Unfortunately, the recovery of heavy metals from this production process was rather limited due to the lack of affordable technologies, and consequently, the produced RM was enriched with heavy metals (Ujaczki et al. 2018; Li et al. 2020).

The spatial variability of selected heavy metals in soils surrounding the RM slag yard is shown in Fig. 1. Total concentrations of Cr, Ni, Cu, As, Cd, Sb, Pb, and Co in soil ranged from 149.36 to 221.95 μg/g, from 68.83 to

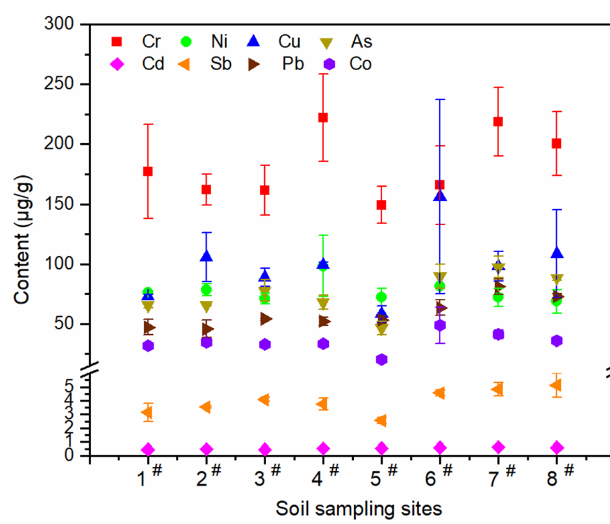

Fig. 1 Spatial distributions of heavy metal contents in soils of Guizhou red mud slag yard

Table 1 Contents (μg/g) of heavy metals in different types of red mud of Guizhou aluminum company

Red mud	Cr	Ni	Cu	As	Cd	Sb	Pb	Co
BRM	418.72 ± 17.43	81.62 ± 1.24	107.88 ± 10.21	57.94 ± 12.80	0.76 ± 0.13	4.46 ± 0.10	144.84 ± 5.33	22.12 ± 0.51
SRM	376.09 ± 19.91	89.71 ± 0.83	122.17 ± 9.92	65.89 ± 2.73	0.71 ± 0.14	3.07 ± 0.00	81.50 ± 4.24	24.51 ± 1.64
CRM	421.19 ± 1.12	86.22 ± 5.00	117.58 ± 8.74	55.76 ± 0.21	0.79 ± 0.00	4.33 ± 0.00	152.71 ± 1.91	22.92 ± 0.30

BRM red muds from Bayer process, *SRM* red muds from sintering process, *CRM* red muds from combined Bayer-sintering process

98.27 μg/g, from 58.22 to 156.16 μg/g, from 46.59 to 97.39 μg/g, from 0.45 to 0.63 μg/g, from 2.57 to 5.13 μg/g, from 45.78 to 80.93 μg/g, and from 20.12 to 48.82 μg/g, respectively. The mean concentrations of heavy metals in soil were much higher than those in the reference soil from Guizhou Province, particularly As and Sb, which exceeded threefold (Cheng et al. 2014). In this study, the mean concentrations of Cr, Ni, Cu, and Co were higher than those reported in soils from Henan and Guangxi provinces, China, affected by bauxite residue (Sun et al. 2015; Guo et al. 2018) and the Ajka RM spill in Hungary (Burke et al. 2012). Meanwhile, it was slightly lower than those reported in seriously polluted soil from abandoned RM dumps, India (Gautam et al. 2018). In terms of As, the content was comparable to that of the Hungarian RM reservoir (Doyle 2010) but higher than that of other RM-contaminated sites (Li et al. 2013).

Notably, the consistency of most heavy metal content sequences (Cr > Cu > Ni > As > Co > Sb) occurred in both RM and the surrounding soils, indicating that RM might be an important pollution source. Moreover, the contents of selected heavy metals in soil exhibited an obvious change trend along the side slope of this RM slag yard as a whole. Cu, Ni, and Cd in the covering soil from the lower part of the slope were much higher than those from the upper part. The rainwaters are almost acidic, and the pH value ranges from 4.6 to 6.9 with a mean of 5.4 (Lü et al. 2017). The easily desorbed fractions of As, Cd, Cr and Cu in RM were leached and migrated under acid rain eluviation, and the mutual transformation between As(III) and As(V) for As and between Cr(III) and Cr(VI) for Cr occurred simultaneously, along with the change in redox conditions (Ghosh et al. 2011).

Relationships of heavy metals in the soil matrix can also provide valuable information on their sources and pathways in the environment. For this purpose, Spearman's rho correlation analysis was performed in this study, and the results are described in Table 2. Significant positive correlations ($p < 0.01$) were observed between As and Sb, As and Co, Cu and Co, and Cd and Pb. There were also significant correlations between Cu and Ni, Pb and As, Pb and Sb, and Sb and Co, while the correlation of Cr with other elements was insignificant. The strong positive correlation among these heavy metals may reflect that they had a common origin and similar pollution levels (Sun et al. 2015). Hence, As, Sb, Pb, Cu, Ni, and Co in soil were mainly derived from the piled RM slag yard and then moved to surrounding areas. Guo et al. (2018) found that Ni, Pb, V, and Zn in soil around a bauxite residue disposal area were highly correlated with Co.

The soil contamination level of heavy metals was comprehensively assessed by the single pollution index, Nemerow's pollution index and the potential ecological risk index using the uncontaminated soil of Guiyang city as a reference and summarized in Tables 3 and 4. The results revealed the order of the single pollution level (expressed as the average P_i) as As (2.76) > Sb (2.41) > Cd (1.70) > Cu and Cr (1.59) > Ni (1.56) > Co (1.46) > Pb (1.42). The soils were heavily polluted by As and Sb, as indicated by the maximum P_i values larger than 3, moderately polluted by Cd, Cr, Ni and Pb ($1 \leq P_i < 3$), and slightly polluted by Co and Cr at site $5^{\#}$ ($P_i < 1$). Overall, this study area was categorized as moderately to severely contaminate based on the range of P_N (1.66–3.19). Heavy contamination ($P_N \geq 3.0$) was recorded at sites $6^{\#}$ and $7^{\#}$. The analysis of P_i and P_N both exhibited a similar spatial tendency: the lower part > the upper part. According to the classification result of P_N (Table 3), approximately a quarter of the sampling points were seriously polluted by heavy metals, slightly lower than the 35% of agricultural soil near Guangxi Province RM slag yard with a mean P_N value of 2.57, and As was also identified as the preferentially controlled heavy metal (Guo et al. 2018). The mean value of E_i for selected heavy metals ranked as Cd > As > Sb > Cu > Ni > Co > Pb > Cr (Table 4). The ecological risks of Cd were at a moderate risk level for all sampling sites, while other heavy metals were associated with relatively low ecological harm. This may be ascribed to the high bioavailability and biotoxicity of Cd, as reflected by its toxicity coefficients of 30 being far greater than those

Table 2 Pearson correlation coefficients of heavy metal contents in soils of Guizhou red mud slag yard

	Cr	Ni	Cu	As	Cd	Sb	Pb	Co
Cr	1	− 0.21	0.135	0.508	0.467	0.536	0.537	0.319
Ni		1	0.811*	0.346	0.343	0.268	0.124	0.691
Cu			1	0.673	0.456	0.671	0.337	0.907**
As				1	0.596	0.957**	0.799*	0.856**
Cd					1	0.636	0.876**	0.469
Sb						1	0.806*	0.767*
Pb							1	0.495
Co								1

* $P < 0.05$ (Double tail)

** $P < 0.01$ (Double tail)

Table 3 Pollution assessment of heavy metals in soils of Guizhou red mud slag yard

Sampling site	P_i								P_N
	Cd	Pb	Cu	Ni	Co	Cr	As	Sb	
1#	1.52	1.27	1.19	1.49	1.38	1.63	2.62	2.11	2.19
2#	1.61	1.24	1.73	1.54	1.50	1.49	2.63	2.36	2.24
3#	1.51	1.46	1.46	1.4	1.42	1.48	3.11	2.73	2.55
4#	1.76	1.41	1.63	1.93	1.45	2.04	2.72	2.51	2.36
5#	1.81	1.44	0.95	1.42	0.87	1.37	1.86	1.72	1.66
6#	2.00	1.71	2.56	1.6	2.12	1.52	3.59	3.05	3.00
7#	2.10	2.19	1.61	1.41	1.79	2.01	3.9	3.23	3.19
8#	2.03	1.97	1.78	1.35	1.56	1.84	3.54	3.42	2.94
Mean	1.70	1.42	1.59	1.56	1.46	1.59	2.76	2.41	2.52

Table 4 Evaluation of the potential ecological risk of heavy metals in soils of Guizhou red mud slag yard

Sampling site	E_i								RI
	Cd	Pb	Cu	Ni	Co	Cr	As	Sb	
1#	45.7	6.37	5.97	7.46	6.9	3.25	26.22	10.56	112.43
2#	48.28	6.19	8.67	7.69	7.52	2.97	26.29	11.82	119.44
3#	45.34	7.32	7.29	6.99	7.12	2.96	31.08	13.63	121.73
4#	52.86	7.05	8.14	9.63	7.26	4.07	27.17	12.53	128.72
5#	54.36	7.22	4.77	7.09	4.37	2.74	18.64	8.58	107.76
6#	59.86	8.57	12.8	7.99	10.61	3.04	35.91	15.23	154.02
7#	62.95	10.94	8.05	7.07	8.96	4.01	38.96	16.16	157.10
8#	60.82	9.86	8.89	6.75	7.8	3.68	35.37	17.1	150.27
Mean	51.07	7.12	7.94	7.81	7.3	3.17	27.55	12.06	124.02

of other metals (Hakanson 1980). The *RI* values of heavy metals in soils were equivalent to those in RM dumps of Guangxi province (Guo et al. 2018), which indicated that the general ecological risk was low to moderate risk level.

Herbs were the most abundant species at the studied sites, which is in line with a prior study that reported that grass accounted for 43.4% of the total plant species around RM dumps of Hindalco Industries Ltd., Renukoot, India, followed by trees at 36.4% and shrubs at 20.2% (Gautam et al. 2018). Herbaceous plants can usually survive more easily in harsh environments than shrubs and woody plants and thus have been preferentially used in metallurgical residue rehabilitation (Gautam et al. 2018). Courtney et al. (2009) found 47 plant species on rehabilitated RM dumps, of which Asteraceae and Poaceae were the dominant families, with 14 species and 9 species, respectively. Furthermore, Poaceae constituted 32.4% of the total herbaceous species, followed by Asteraceae (24.3%) and Euphorbiaceae (8.1%) (Gautam and Agrawal 2019).

The contents of heavy metals in the whole plants and different tissues at the RM slag yard are presented in Fig. 2. The mean contents of heavy metals in the entire plant decreased in the order of Cr (11.28 μg/g) > Cu (8.12 μg/g) > Ni (5.54 μg/g) > Pb (0.71 μg/g) > Co (0.40 μg/g) > As (0.25 μg/g) > Cd (0.20 μg/g) > Sb (0.14 μg/g). Considerable amounts of Cr, Ni and Cu were detected in *Conyza canadensis* and *Coriaria sinica*, while other plants were relatively low (Fig. 2a). The contents of Cu, Ni, As, and Cd in the plant were below the phytoxic threshold (Cu = 20–100 μg/g, Ni = 10–100 μg/g, As = 5–20 μg/g, Cd = 5–30 μg/g dry matter; Kabata, 2011) for all sampling sites, whereas Cr exceeded the lowest critical toxic values (Cr = 5–30 μg/g dry matter). Moreover, the concentrations of heavy metals in different plant tissues are also shown in Fig. 2b, c, and d. Overall, the contents of Cr, As, Sb, Pb Ni, Cd and Co in the leaves were comparably higher than those in the roots and stems of *Artemisia argyi* and *Conyza canadensis*, whereas *Cosmos bipinnata* had the opposite trend, with a high content of heavy metals in the roots. Overall, the contents of Cr, Ni and Cu were much higher than those of other heavy metals in different vegetation tissues. Various plant species possess different strategies for metal uptake and allocation, as well as metal tolerance (Li et al. 2015). For example, *Conyza canadensis* and *Coriaria sinica* have a higher enrichment capacity for heavy metals than other plants, particularly Cr, Ni and Cu (Fig. 3a). *Conyza canadensis* was identified as a suitable species for heavy metal phytoremediation, especially for Cr, Ni, Cu, and Pb pollution (Irshad et al. 2015). *Coriaria nepalensis* was also observed as an effective bioindicator of heavy metal contamination derived

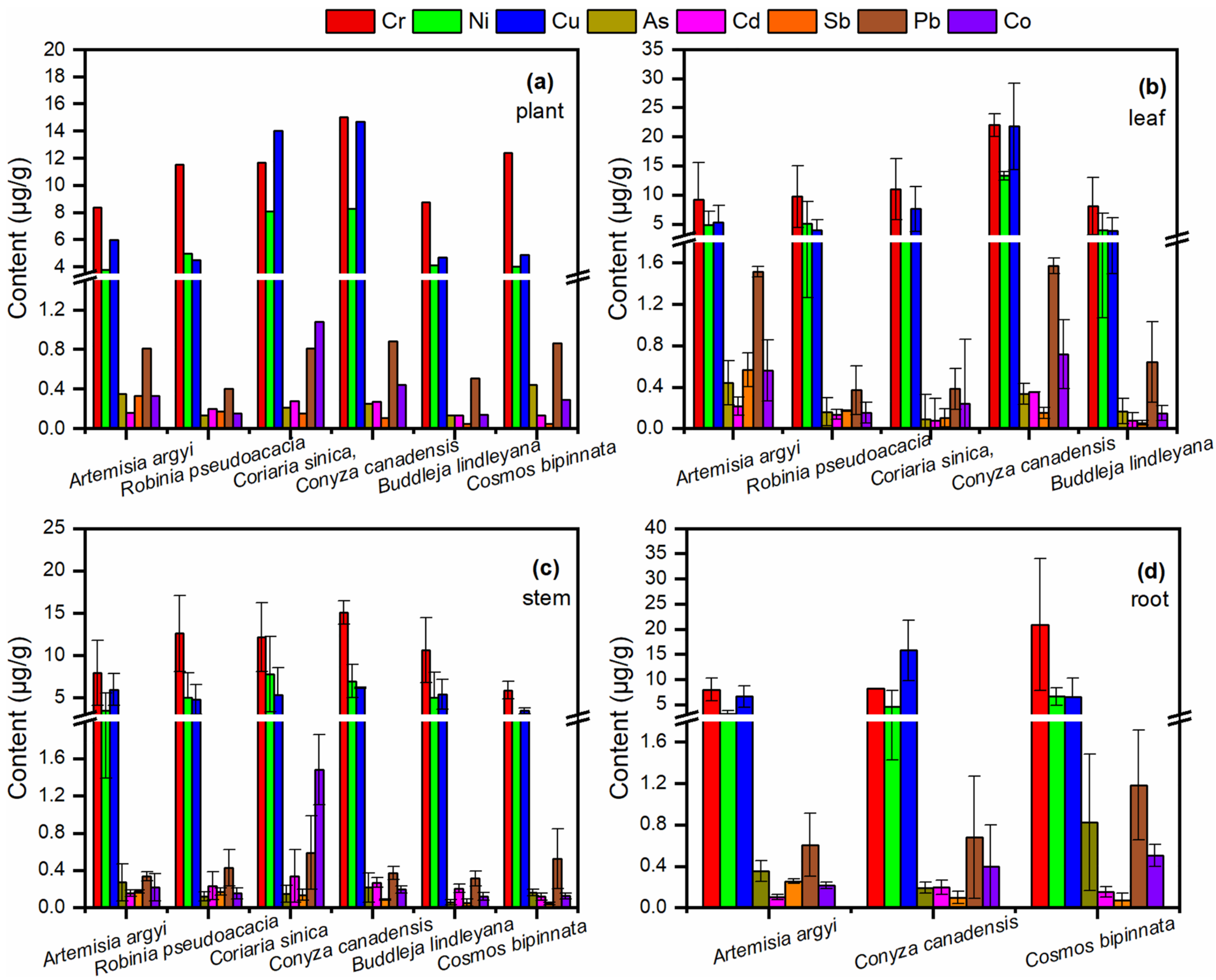

Fig. 2 Contents of heavy metals in whole plants and different tissues from Guizhou red mud slag yard: **a** entire plant; **b** leaf; **c** stem; **d** root

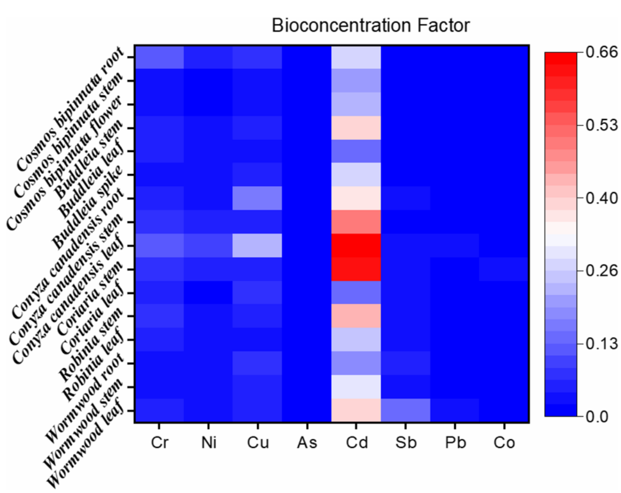

Fig. 3 Bioconcentration factors of heavy metals in whole plants from Guizhou red mud slag yard

from abandoned karst bauxite in Southwestern China (Wang and Zhang 2020).

To compare the phytoaccumulation ability of heavy metals, the *BCF* and *TF* factors were determined for different plant species. A *BCF* value > 1 indicates that a particular metal element is more accumulative in plants relative to environmental pollution, while a *BCF* value < 1 indicates a metal excluder (Gautam and Agrawal 2019). In the present study, all dominant plant species exhibited lower BCF values (Fig. 3), suggesting that no plant species was identified as a hyperaccumulator. The *BCF* value of Cd was the highest among the selected heavy metals for all plants and organs, which agreed with Ismael et al. (2019). Pontederiaceae and Gramineae showed rather higher tolerance for Cd, owing to Cd detoxification mechanisms and defense strategies through increased antioxidant enzyme activity and gene regulation (Li et al. 2015). Additionally, if the *TF* values of plants are more than 1, this implies that this kind of plant can be

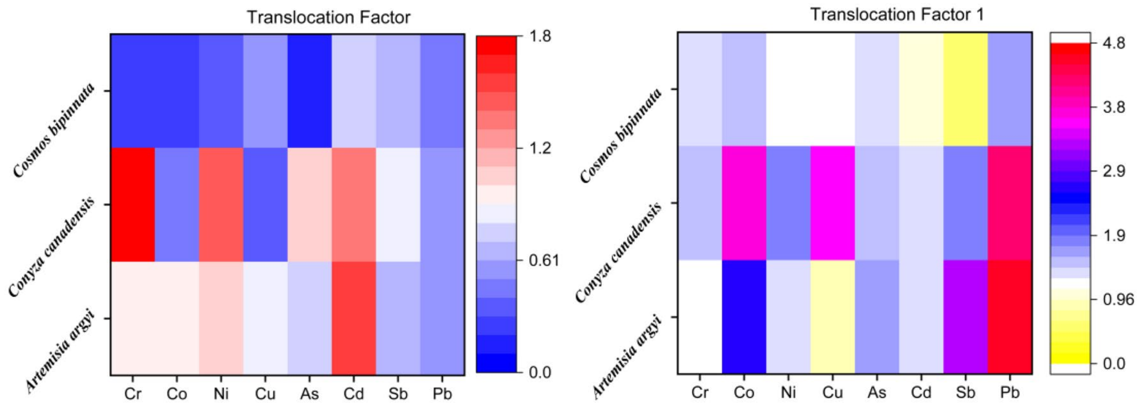

Fig. 4 Translocation factors of heavy metals between plant tissues from the Guizhou red mud slag field: **a** from root to stem; **b** from stem to leaf

considered a suitable candidate for heavy metal accumulation, while plants with *TF* < 1 can be used for phytostabilization. As seen from Fig. 4a and b, *Artemisia argyi* and *Conyza canadensis* have a greater ability to transport heavy metals both from the root to the stem and from the stem to the leaf than *Cosmos bipinnata*. For a single heavy metal, the value of TF_1 was almost higher than that of *TF* for these three plants above. In particular, *Conyza canadensis L.* showed a strong transport capacity for Cr from the root to the stem with a *TF* value of 1.84. The TF_1 values of most heavy metals were above 1, except Cu for *Artemisia argyi* and Sb for *Cosmos bipinnata*, reflecting that these two metals readily accumulate in the stem. In contrast, the *TF* values of heavy metals were always below 1 for *Cosmos bipinnata*, which indicated that this species might be a potential candidate plant for phytostabilization. In other words, it is capable of fixing the heavy metals in the roots, thus reducing the translocation of metals to ground plant parts. Mishra et al. (2017) found that *Saccharum bengalense* Retz. retained Cr, Pb, Cu and Mn in the root part and served as a promising species for the remediation of RM deposits. Most herbaceous species exhibited *TF* values greater than 1 for Ni, Cd, and Pb, while *B. mutica* and *E. cynosuroides* had lower *TF* values (< 1) for Co and Cr (Gautam and Agrawal 2019). It was reported that *Cosmos bipinnata* can grow well on Cd-contaminated soil with rather low *TF and TF1* results and can be used for Cd phytostabilization in overburden dumps (Huang et al. 2017).

Furthermore, Pearson correlation analysis was performed to clarify the utilization processes of heavy metals by plants (Table S4 and S5). Significant positive correlations between Ni and Cd and positive correlations between Cr and Ni and Cr and Cd were observed in the stem. In contrast, more correlations presented between Cr and Cu, between Co and Cd, between Co and Pb, between Ni and Cu, and between As and Pb in the leaf, which suggested that these pairs of heavy metals share some mechanisms during the transport processes or mutual dependence. The synergistic accumulation effect of these metals is more remarkable in leaves than in other tissues for the contaminated site, supported by the higher *TF1* results of most heavy metals, except for Sb (Fig. 4b). However, the bioavailability of heavy metals within the studied rehabilitated site and potential mechanisms of food chain transfer are still unclear. These areas need careful study before definitive statements can be made regarding the sustainability of RM disposal field rehabilitation strategies (Chauhan and Ganguly 2011; Gautam and Agrawal 2019).

Supplementary Information The online version contains supplementary material available at https://doi.org/10.1007/s00128-022-03493-8.

Acknowledgements This study was supported by the National Key Research and Development Program of China (2018YFC1903500), Special Fund of Governor of Guizhou Province ([2012]7), and Guizhou Province Science and Technology Fund ([2019]5410).

References

Ahmadnejad F, Zamanian H, Taghipour B et al (2017) Mineralogical and geochemical evolution of the Bidgol bauxite deposit, Zagros Mountain Belt, Iran: implications for ore genesis, rare earth elements fractionation and parental affinity. Ore Geol Rev 86:755–783

Burges A, Alkorta I, Epelde L et al (2018) From phytoremediation of soil contaminants to phytomanagement of ecosystem services in metal contaminated sites. Int J Phytoremediation 20(4):384–397

Burke IT, Mayes WM, Peacock CL et al (2012) Speciation of arsenic, chromium, and vanadium in red mud samples from the ajka spill site, Hungary. Environ Sci Technol 46:3085–3092

Chauhan S, Ganguly A (2011) Standardizing rehabilitation protocol using vegetation cover for bauxite waste (red mud) in eastern India. Ecol Eng 37:504–510

Cheng H, Li K, Li M et al (2014) Geochemical background and baseline value of chemical elements in urban soil in China. Earth Sci Front 21(3):265–306

Courtney R, Mullen G, Harrington T (2009) An evaluation of revegetation success on bauxite residue. Restor Ecol 17(3):350–358
Di Carlo E, Boullemant A, Courtney R (2019) A field assessment of bauxite residue rehabilitation strategies. Sci Total Environ 663:915–926
Di Carlo E, Boullemant A, Courtney R (2020) Ecotoxicological risk assessment of revegetated bauxite residue: Implications for future rehabilitation programmes. Sci Total Environ 698:134344
Doyle P (2010). Hungary toxic disaster—entire villages to be abandoned.
Flora Reipublicae Popularis Sinicae (Flora of China) (2014) Science Press, Beijing
Gautam M, Agrawal M (2019) Identification of metal tolerant plant species for sustainable phytomanagement of abandoned red mud dumps. Appl Geochem 104:83–92
Gautam M, Pandey B, Agrawal M (2018) Identification of indicator species at abandoned red mud dumps in comparison to residential and forest sites, accredited to soil properties. Ecol Indicat 88:88–102
Ghosh I, Guha S, Balasubramaniam R et al (2011) Leaching of metals from fresh and sintered red mud. J Hazard Mater 185(2–3):662–668
Guo Y, Li YB, Xue SG et al (2018) Risk analysis of heavy metal contamination in farmland soil around a bauxite residue disposal area in Guangxi. Environ Sci 39(7):3349–3357 ((**in Chinese with English abstract**))
Hakanson L (1980) An ecological risk index for aquatic pollution control. A Sedimentological Approach Water Res 14(8):975–1001
Huang JJ, Yang ZB, Li JH et al (2017) Cadmium accumulation characteristics of the floricultural plant Cosmos bipinnata. J Chem Ecol 33(9):807–816
Inzar-Sekuli J, Stamenkovi UM, Tomovi G et al (2019) Assessment of trace element accumulation potential of Noccaea kovatsii from ultramafics of Bosnia and Herzegovina and Serbia. Environ Monit Assess 191:540
Irshad M, Ahmad S, Pervez A et al (2015) Phytoaccumulation of heavy metals in natural plants thriving on wastewater effluent at Hattar industrial estate. Pakistan Int J Phytoremediation 17(2):154–158
Ismael MA, Elyamine AM, Moussa MG et al (2019) Cadmium in plants: uptake, toxicity, and its interactions with selenium fertilizers. Metallomics 11:255–277
Kabata-Pendias A (2011) Trace Elements in Soils and Plants, 4th edn. CRC Press, Taylor and Francis Group
Li YR, Wang J, Su Y et al (2013) Evaluation of chemical immobilization treatments for reducing arsenic transport in red mud. Environ Earth Sci 70:1775–1782
Li J, Yu H, Luan Y (2015) Meta-analysis of the copper, zinc, and cadmium absorption capacities of aquatic plants in heavy metal-polluted water. Int J Environ Res Public Health 12:14958–14973
Li Q, Peng D, Zheng W et al (2020) Attenuation of Cr/Pb in bauxite leachates by bentonite–polymer composite geosynthetic clay liners. RSC Adv 10:44672–44678
Lü P, Han GL, Wu QX (2017) Chemical characteristics of rainwater in karst rural areas, Guizhou Province, Southwest China. Acta Geochimica 36:572–576
Mayes WM, Burke IT, Gomes HI et al (2016) Advances in understanding environmental risks of red mud after the Ajka spill. Hungary J Sustain Metall 2(4):332–343
Mišík M, Burke IT, Reismüller M et al (2014) Red mud, a byproduct of aluminum production, contains soluble vanadium that causes genotoxic and cytotoxic effects in higher plants. Sci Total Environ 493:883–890
Ren J, Chen J, Han L et al (2018) Spatial distribution of heavy metals, salinity and alkalinity in soils around the bauxite residue disposal area. Sci Total Environ 628:1200–1208
Sun X, Ning P, Tang XL et al (2015) Heavy metals pollution assessment in soil surrounding red mud ponds in Shaanxian. Henan. Journal of Northwest Agricutural&forestry University 43(5):122–128 ((**in Chinese with English abstract**))
Ujaczki E, Feigl V, Molnár M et al (2018) Reusing Bauxite Residues: Benefits Beyond (Critical Raw) Material Recovery. J Chem Technol Biotechnol 93:2498–2510
Wang DF, Zhang ZH (2020) Higher plants as bioindicators of metal contamination from Shangdong abandoned karst bauxite, southwestern China. Plant Biol 22:323–330
Xue S, Kong X, Zhu F et al (2016) Proposal for management and alkalinity transformation of bauxite residue in China. Environ Sci Pollut Res 23(13):12822–12834
Yang DZ, Deng WW, Tan A et al (2021) Protonation stabilized high As/F mobility red mud for Pb/As polluted soil remediation. J Hazard Mater 404:124143